JME

Journal of Mining & Environment,
Vol.8, No.2, 2017, 191-201.
DOI: 10.22044/jme.2016.661

Technical Note

Mineralogical and physical beneficiation studies for iron extraction from Bardaskan titanomagnetite placer deposit

M. Hosseinzadeh[1*], M. Alizadeh[1], M.R. Hosseini[2]

1. Materials and Energy Research Center (MERC), Karaj, Iran
2. Department of Mining Engineering, Isfahan University of Technology, Isfahan, Iran

Received 1 January 2016; received in revised form 25 June 2016; accepted 7 August 2016
**Corresponding author: mta.hosseinzadeh@yahoo.com (M. Hosseinzadeh).*

Abstract

In this work, a bench-scale process was developed using mineral-processing methods to recover iron from a placer deposit located in Bardaskan, Khorasan-e-Razavi, Iran. The mineralogical studies were performed by X-ray Diffraction (XRD), X-ray Fluorescence (XRF), Electron Probe Micro-Analyzer (EPMA), and an optical microscope. These studies indicated that titanomagnetite, magnetite, and hematite were presented in the sample as valuable minerals. In contrast, the gangue minerals were silicates such as pyroxene, plagioclase, quartz, feldspar, calcite, and some secondary minerals. The optimum liberation degree of the iron-containing minerals was obtained to be 75 µm with average Fe and TiO_2 contents of 5% and 1%, respectively. The analysis showed that magnetite was the main iron mineral, and most of the hematite was formed due to martitization. Also minor ilmenite contents were found in hematite and magnetite in a blade form. The maximum TiO_2 content in the magnetite lattice was 19%, only 8% of which was recovered to the magnetic product. Eventually, an iron concentration flow sheet was developed, which included the removal of a major part of silicates and then iron minerals by a low intensity wet magnetic separator. The final product contained 55, 7.8, and 0.77% of Fe, TiO_2, and V_2O_5, respectively, which can be used for iron production, and V_2O_5 extraction (as the by-product).

Keywords: *Titanomagnetite, Magnetite, Liberation Degree, Iron, Flow Sheet.*

1. Introduction

Titanomagnetites are found in numerous titaniferous deposits as well as placer iron ore deposits spread all over the globe. They are present mainly in ores as iron oxide minerals beside magnetite or often join igneous intrusions of basic rocks, primarily anorthosites. The main associated minerals are plagioclase, amphiboles, augite, apatite, pyroxene, and olivine. In the recent years, an increasing interest has been observed for exploiting these resources and producing their marketable products such as iron and steel, titanium dioxide concentrates, vanadium, and concentrates of pyrites and non-ferrous metal sulfides [1]. The titanmagnetite ore consists of two main phases: ilmenite ($FeTiO_3$, 52.65% TiO_2 and 47.35% FeO) and magnetite (Fe_3O_4, 68.97% Fe_2O_3 and 31.03% FeO) with some ilmenite dissolved in the magnetite matrix. Vanadium is dissolved in magnetite as V_2O_3 that replaces Fe_2O_3 [1, 2].

Titanomagnetites are a source of titanium, vanadium, and iron. Indeed, most of the world's vanadium production originates from the titanomagnetite ores [3]. At the present time, titanium is mainly recovered from ilmenite and rutile concentrates, which contain between 50 and 97% TiO_2 [4, 5]. Ilmenite is the most common source of titanium dioxide (TiO_2) [6], which is widely used for the production of a white pigment [7].

The amenability of various iron-titanium deposits to beneficiation is controlled by the mineralogical and textural characteristics. In the evaluation of mineralization and design of the mineral dressing

procedures, the distribution of valuable materials is a matter of concern, and it is necessary to determine whether a given element has occurred in one mineral or several minerals [8].

Tellnes [9] and Bjerkreim-Sokndal [10] in Norway, Kauhajärvi [11], Lumikangas [12], Koivusaarenneva [8, 13], Iso-Kisko [14], Otanmäki [15] and Kalviä [16] in Finland, Sinarsuk V-Ti project in West Greenland [17], the Sept-Iles project in Canada [18], and Navaladi and Surungudi area in southern India [19] are some of the most important titanomagnetite deposits that have been investigated from an applied mineralogical viewpoint.

The placer deposits are considered to be the economically viable ones because of their profitability and easy mineability. In comparison with rutile, ilmenite concentrates have a lower titanium content (less than 52.6% of TiO2) and a significant amount of Fe [23-25].

Some titaniferous ores are high enough in iron content to allow further processing directly after milling [1, 20-22]. However, most of the ores have to be upgraded, in particular, when the ores contain vanadium, ilmenite, and other valuable components. Generally, upgrading the titaniferous ores includes primary and secondary crushing, two to three grinding stages, and magnetic separation. Some of the ores can be adapted to autogenous grinding, which substantially decreases the costs compared to rod mill or ball mill grinding. The magnetite and titanomagnetite concentrate produced also contains a considerable amount of vanadium. Ilmenite and pyrite are separated with the non-magnetic fraction, and are then recovered by selective flotation in separate marketable products [1].

The Bardaskan titanomagnetite deposit is located about 20 Km from SW of Bardaskan, nearby Sharif-Abad village, Khorasan-e-Razavi, Iran. This deposit has been identified as a titaniferous resource. The geological and petrological studies on the region indicate that quaternary deposits are scattered on a massive scale. These deposits are new and old aeolian sand sediments. Deposits older than quaternary have not been found in the region. Also this ore can be found in alluvial and aeolian deposits in the hilly region, which have concentrated in the quaternary deposits for the effects of wind and flooding. This process has mainly occurred in the hills located in the wind and waterway directions, so the iron ore is concentrated largely in some parts of the waterways. Due to the concentration of minerals mainly by wind, grains are uniform in a sand size.

In the present work, the mineralogical and microscopic studies were performed, and the quality and quantity of the liberated minerals of the Bardaskan deposit were investigated. Initially, a high-intensity dry magnetic separator (HIDMS) was used. Then the liberation degree of the valuable mineral and trace elements were estimated, and the distribution and dispersion of iron, titanium, and vanadium were identified. Finally, the grinding, gravity, and magnetic methods were used to achieve an optimum separation of iron, a flow sheet was developed for upgrading the mineral, and the process was investigated from an economical viewpoint.

2. Materials and method

2.1. Sampling and X-ray characterization

The ore used in this study was supplied from a placer deposit located in Bardaskan, Khorasan-e-Razavi, Iran. The mineralogical characterization of the samples was carried out by an X-ray diffraction (XRD) Philips X'Pert PRO equipped with a 2.5 kW cobalt X-ray tube (λ = 1.789010 Å) and a gas detector in the atmosphere. The current and voltage were 35 mA and 40 kV, respectively, and the radiation angle (2θ) was set between 4 and 85 degrees. The chemical composition of the samples was determined by an X-ray fluorescence (XRF) Philips MagiX PRO equipped with a 4 kW rhodium tube and LiF 200 crystals in vacuum. Voltage, current, and angle (2θ) were set at 50 kV, 56 mA, and 51.67^o, respectively, for iron with duplex detector, 28 kV, 95 mA, and 86.17^o, respectively for titanium with gas detector, and 37 kV, 70 mA, and 76.99^o, respectively, for vanadium with duplex detector. The mineralogical and chemical analyzes of the iron ore are presented in Tables 1 and 2, respectively. According to the chemical analysis of the placer sample, the initial sample is low in iron, and much of the deposit is composed of silica and non-iron minerals.

2.2. Preconcentration and sieve analysis

To obtain a high grade concentrate, firstly, the placer mineral was separated by a high-intensity dry magnetic separator (HIDMS) in a magnetic field of 13500 G, particle size minus 2 mm, and dried, and then was divided into four size ranges of +500-1000, +300-500, +150-300, and +75-150 µm. Afterwards, further mineralogical studies and other beneficiation steps were performed on the prepared size fractions.

Table 1. Mineralogical composition of placer iron ore sample.

Mineral	Chemical formula
Augite	$(Ca,Na)(Mg,Fe,Al,Ti)[(Si,Al)_2O_6]$
Albite	$NaAlSi_3O_8$
Quartz	SiO_2
Hematite	Fe_2O_3
Magnetite	$Fe^{2+}Fe^{3+}{}_2O_4$
Diopside	$MgCaSi_2O_6$
Calcite	$CaCO_3$
Muscovite	$KAl_2(AlSi_3O_{10})(OH)_2$
Montmorillonite	$(Na,Ca)_{0.33}(Al,Mg)_2(Si_4O_{10})(OH)_2 \cdot nH_2O$
Tremolite	$Ca_2Mg_5Si_8O_{22}(OH)_2$

Table 2. Chemical analysis of placer iron ore sample.

Element/Oxide	Fe	TiO_2	V_2O_5	SiO_2	Na_2O	CaO	MgO	K_2O	Al_2O_3
Percent	5.2	1.0	0.1	53.0	6.1	6.3	5.3	3.2	15.3

2.3. Mineralogical studies

Thin and polished cross-sections were prepared from four size fractions of the first separation concentrate, and were used to study the textural relationship of samples by reflected and transmitted optical microscopy using a polarized optical Zeiss microscope (model: Axioplan2). Also in order to describe the inclusion, exclusion, and other textural relationships, an Electron Probe Micro Analysis (EPMA, model: Cameca SX100) was applied. The device was calibrated using titanium on ilmenite, iron on specularite, calcium and silicon on wollastonite, vanadium on pure vanadium, chromium on chromite, magnesium on periclase, and aluminum on corundum. The specimens were analyzed in 15-20 seconds using a current of 20 nA with an acceleration voltage of 15 keV, and the electron beam of 2-5 μm in size. Moreover, in order to obtain the liberation degree, a microscopic counting method was used. In this method, the free and locked minerals of magnetite, hematite, and titanomagnetite existing in the polished sections were counted using a polarized microscope, and calculated by the following equation:

$$ld = \frac{n_1}{n_1 + n_2} \times 100 \quad (1)$$

where ld is the liberation degree, and n_1 and n_2 are the numbers of free and lock grains, respectively.

3. Results and discussion

The size analysis of the feed and the concentrate derived from the first separation process are depicted in Figure 1. Also the XRD analysis and chemical composition of the samples from the concentrate and tailing of HIDMS are shown in Tables 3 and 4, respectively.

According to these tables, most of the minerals present in the tailing are silicates, which indicates that the magnetic method applied for the separation of non-iron and invaluable minerals has been effective. Considering the low iron content of the ore, it was found that the iron compounds locked in the coarse particles have lowered the concentrate assay and separation efficiency, which may be improved by applying an appropriate beneficiation process. Comparing the different compositions in the concentrate and tailing (Table 4), it can be said that due to the inclusion of SiO_2 and Al_2O_3 in iron-bearing minerals, the composition of concentrate and tailing are the same after magnetic separation. The low iron assay of the concentrate may be increased by decreasing the particle size and designing an appropriate processing circuit. Finally, the titanium and vanadium contents of the samples were low in contrast to the titanomagnetic minerals.

3.1. Microscopic studies of polished sections

Studies performed on the concentrate sample indicate that most of the particles have signs of erosion, like smooth corners, and semi-round to round shapes that reveal carrying in short and moderate paths. The main mineral observed is quartz, which is in the form of round crystals or fine crystal cherts. The second abundant mineral is plagioclase, which is less round and is altered to muscovite and quarts due to weathering. After that, there is pyroxene, which is as round and weathered as plagioclase. They have a close relationship to each other, and also to magnetite and hematite (the main minerals). Weathering of pyroxene causes the formation of secondary minerals like calcite and clays. As it can be seen

in Figures 2 and 3, secondary calcite along with plagioclase, pyroxene, and magnetite are present in the sample, and the crystals are larger and less round. Hematite is the most abundant metallic mineral of the sample. Table 5 introduces the abbreviations used to mark minerals in the thin and polished section images.

Most hematites are formed as a result of martitization. Martitization has generated hematite blades between the crystal surfaces of magnetite. In addition, there are some blades of ilmenite and titanomagnetite. The amounts of hematite and magnetite in the initial concentrate sample are 10% and 5%, respectively. Also a minor ilmenite content was found with hematite and magnetite in the blade form. Moreover, although free ilmenite was not observed in the sample, less than 2% of titanomagnetite was occasionally found as co-growth with magnetite.

Using thin sections prepared from the HIDMS concentrate, the results of the studies on the liberation degree are listed in Table 6. It can be deduced that most of the involvements are in contact modes (between metallic minerals and tailing), inclusions, and blades in tailing minerals (Figures 4 and 5). Also the size of many of these inclusions is less than 0.1 mm. Magnetite is accompanied mostly by pyroxene, and then plagioclase. The relations of these minerals are so that the inclusions of magnetite in tailing, and vice versa, are discernable. Furthermore, ilmenite blades are widely observable in magnetite, and hematite formation between crystal surfaces and cleavages of magnetite caused by martitization makes it difficult to differentiate between them. In conclusion, a particle size of minus 75 µm was selected to achieve an optimum separation in the final magnetic process.

3.2. Liberation degree studies

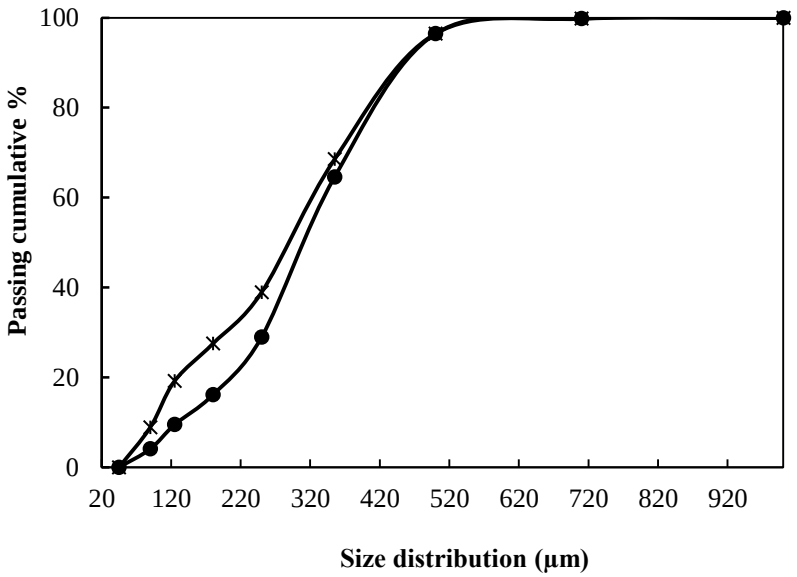

Figure 1. Passing cumulative percentage of feed and concentrate of HIDMS (* Before separation, • After separation).

Table 3. Mineralogical composition of HIDMS concentrate and tailing by XRD method.

Mineral	Major phases		Minor phases	
Concentrate	Quartz	SiO_2	Hematite	Fe_2O_3
	Anorthite	$CaAl_2Si_2O_8$	Montmorillonite	$(Na,Ca)_{0.33}(Al,Mg)_2(Si_4O_{10})(OH)_2 \cdot nH_2O$
	Diopside	$MgCaSi_2O_6$		
	Albite	$NaAlSi_3O_8$	Tremolite	$Ca_2Mg_5Si_8O_{22}(OH)_2$
	Augite	$(Ca,Na)(Mg,Fe,Al,Ti)[(Si,Al)_2O_6]$	Muscovite	$KAl_2(AlSi_3O_{10})(OH)_2$
	Magnetite	$Fe^{2+}Fe^{3+}{}_2O_4$		
Tailing	Calcite	$CaCO_3$	(α-Quartz)	SiO_2
	Crystobalite	SiO_2	Hematite	Fe_2O_3
	Feldspar			

Table 4. Chemical composition of HIDMS concentrate and tailing.

Weight percentage / Element/Oxide	Concentrate wt%	Tailing wt%
Fe	6.54	1.51
TiO_2	1.22	-
SiO_2	47.30	39.04
CaO	7.21	17.72
Al_2O_3	14.80	13.30
MgO	4.81	2.00
Na_2O	5.52	14.81
K_2O	2.53	-
V_2O_5	0.24	-
C	0.11	2.64
S	-	0.01
P	0.21	-
LOI	2.10	10.79

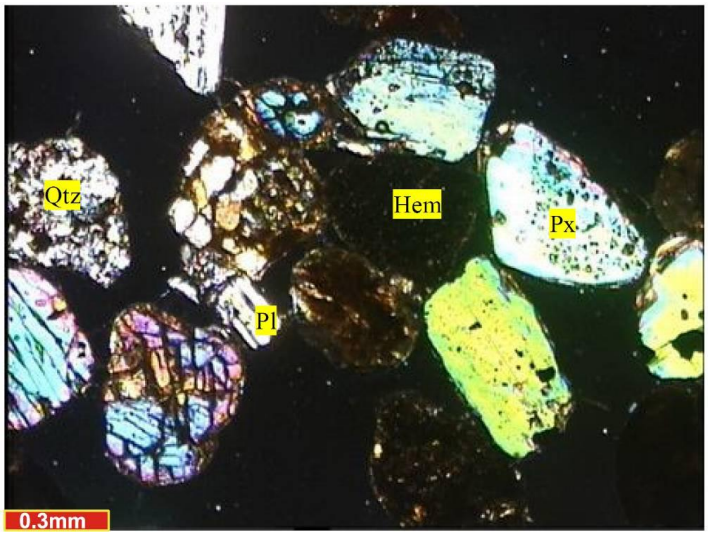

Figure 2. Polished section image showing semi-round particle consisting of pyroxene, quartz, and plagioclase.

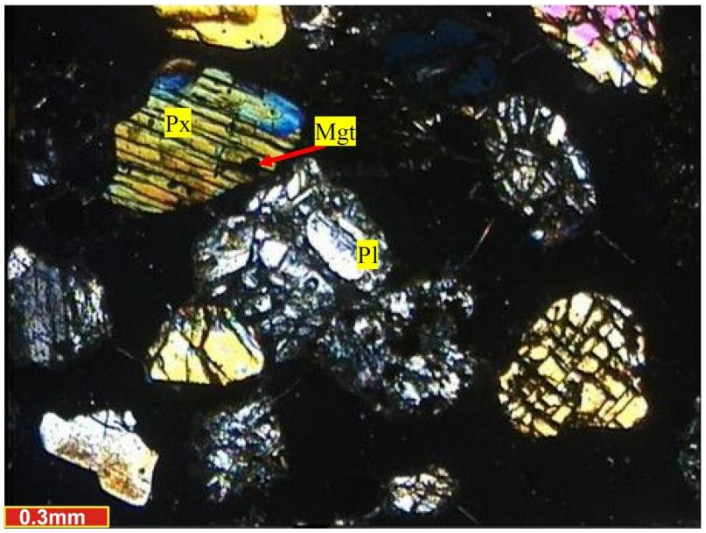

Figure 3. Polished section image showing plagioclase beside pyroxene with magnetic inclusion.

Table 5. Abbreviations used for minerals presented in section images.

Symbol	Chemical formula	Name
Px	$CaMg(SiO_3)_2$	Pyroxene
Pl	$NaAlSi_3O_8$	Plagioclase
Qtz	SiO_2	Quartz
Hem	Fe_2O_3	Hematite
Mgt	$Fe^{2+}Fe^{3+}{}_2O_4$	Magnetite
Gt	α-$Fe^{3+}O(OH)$	Goethite
Gan	-	Gangue

Table 6. Liberation degree of each size fraction.

Particle size (µm)	Magnetite, Hematite, Titanomagnetite	
	Free (%)	Locked (%)
–1000+500	10	90
–500+300	25	75
–300+150	73	27
–150+75	83	17

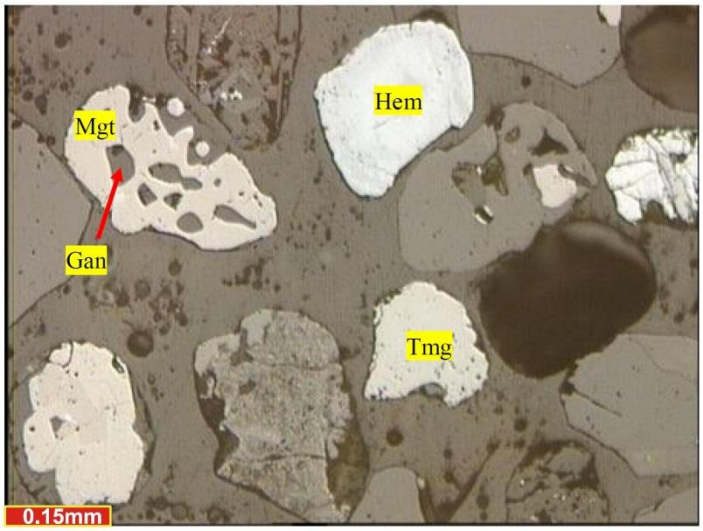

Figure 4. Free and martitized magnetite with titanmagnetite in size range of +150-300 µm (PPL reflective light).

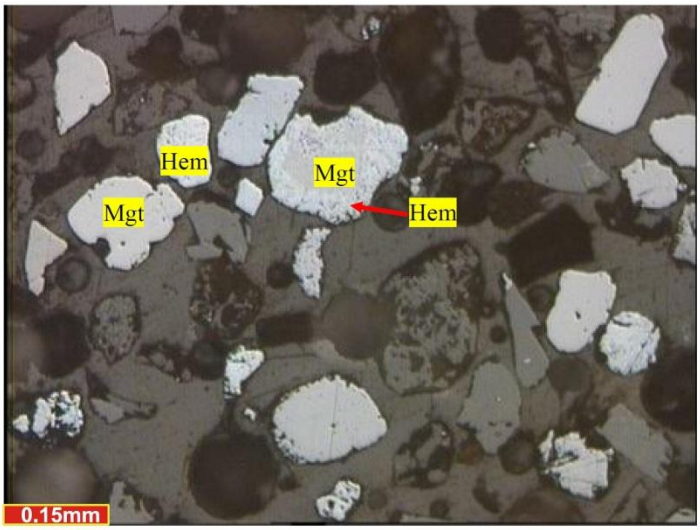

Figure 5. Free semi-round magnetite and hematite with martitized magnetite in size range of +75-150 µm (PPL reflective light).

3.3. EPMA studies on placer sample

Complementary studies on the distribution and dispersion of iron, titanium, and vanadium in iron-bearing minerals using Electron Probe Micro Analysis are shown in Figures 6(a) and 6(b). Figure 6(a) proves the presence of titanomagnetite and a little amount of ilmenite. Also this indicates that the complete liberation of ilmenite from the magnetite cannot be achieved even after fine grinding, which agrees with the findings of other investigators [3, 4]. Additionally, X-ray mapping (also called element mapping) was used to show the diffraction pattern of iron, titanium, and vanadium on the mineral surface (Figure 6(b)). There is a qualitative chemical analysis for each element, which is arranged from low to high and black to red. The closer to red, the higher is the quantity of the element in the region. The back-scattered electron (BSE) images for magnetite, hematite, spinel, and ilmenite are shown in Figures 7 and 8. Different points of BSE image obtained by EPMA in Figures 6(a), 7 and 8 were analyzed using a wavelength dispersive X-ray spectroscopy (WDS) analyzer, and reported in Tables 7 and 8.

Regarding the titanium distribution in iron-bearing minerals and formation of titanomagnetite networks, and with respect to the conditions of iron concentrate comminution (to under 75 μm) in the pellet making process, separation of ilmenite from magnetite seems to be impossible.

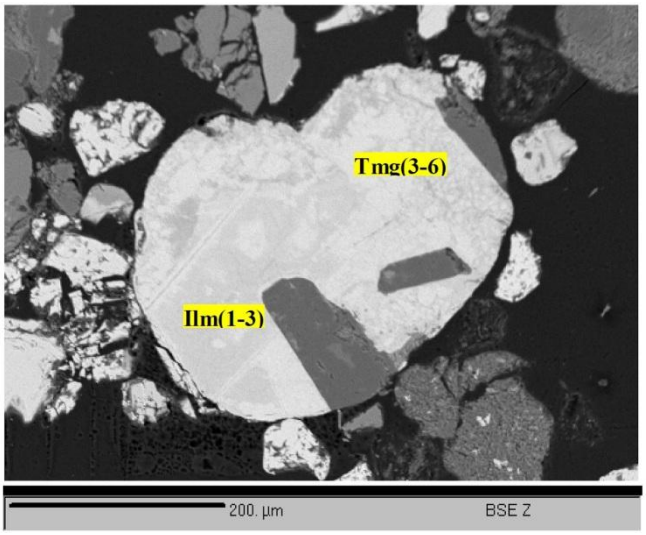

Figure 6(a). BSE image of a thin section obtained by EPMA showing titanomagnetite and ilmenite in placer iron ore.

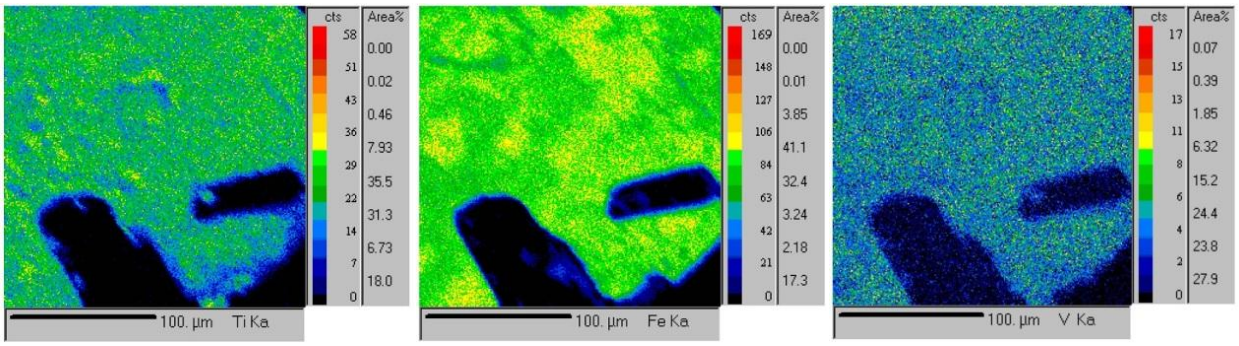

Figure 6(b). Characteristic X-ray maps obtained by EPMA present distribution of Fe, Ti, and V in area specified in Figure 6-a.

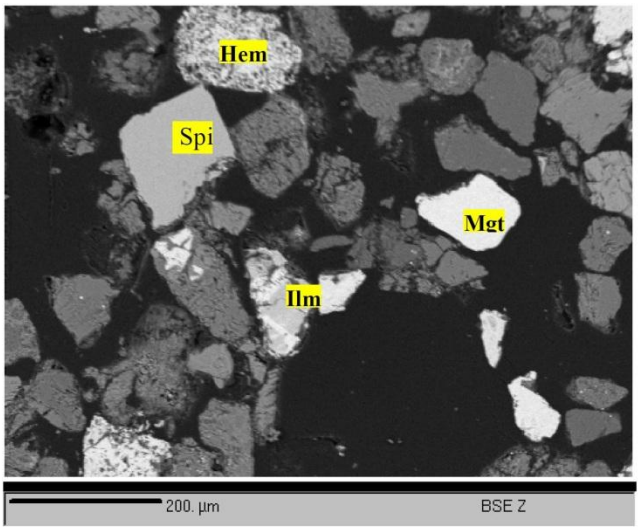

Figure 7. BSE image of a thin section obtained by EPMA showing magnetite, hematite, spinel, and ilmenite in placer iron ore.

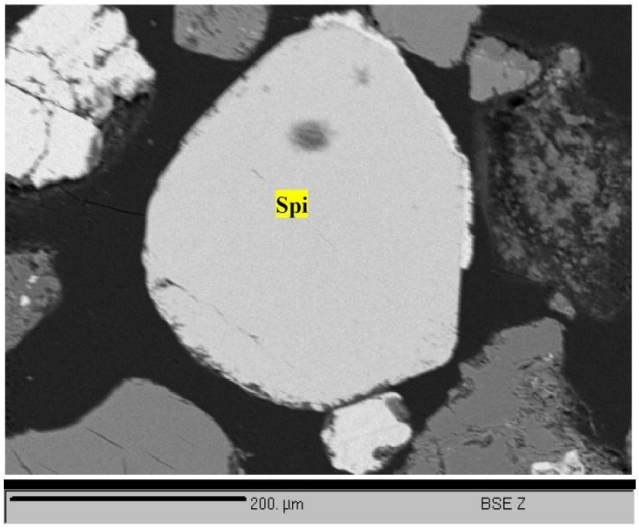

Figure 8. BSE image of a thin section obtained by EPMA showing spinel in placer iron ore.

Table 7. Point chemical analysis of areas detected in Figure 6-a.

Formula	MgO	CaO	FeO	Fe_2O_3	Al_2O_3	V_2O_3	Cr_2O_3	TiO_2
1 / 1.	0.13	6.45	26.89	62.43	0.87	1.02	0.03	0.00
2 / 1.	0.00	8.41	37.08	30.55	1.07	0.94	0.01	18.91
3 / 1.	0.01	8.48	44.36	26.53	0.43	0.77	0.04	18.78
4 / 1.	0.15	1.41	49.92	26.56	1.05	0.99	0.04	16.71
5 / 1.	0.17	0.11	49.91	30.54	0.83	0.95	0.02	15.94

Table 8. Point chemical analysis of spinels detected in Figures 7 and 8.

Formula	MgO	CaO	FeO	Fe_2O_3	Al_2O_3	V_2O_3	Cr_2O_3	TiO_2
7 / 1.	1.20	0.03	44.67	41.01	2.61	0.81	0.01	8.56
8 / 1.	1.30	0.01	45.85	40.38	2.57	0.92	0.02	9.40
9 / 1.	0.26	0.37	41.79	46.72	1.72	0.54	0.04	5.15
10 / 1.	13.74	0.01	14.34	0.57	21.56	0.26	48.69	0.00
11 / 1.	13.42	0.01	14.65	0.07	21.28	0.27	49.00	0.00
12 / 1.	13.60	0.01	14.38	0.05	21.28	0.21	49.31	0.00

3.4. Pilot plant studies

The proposed processing circuit for the enrichment of iron contents of the placer mineral and its associated results and calculations (feed rate considered as 100 kg/h) are depicted in Figure 9. Initial enrichment by HIDMS (under 1 mm) obtains a concentrate containing 6.5% Fe, 1.2% TiO_2, and 0.2% V_2O_5. Afterward, the separation process on the produced concentrate continues, as shown in Figure 9. At last, a magnetite product containing 55% Fe, 7.8% TiO_2, and 0.77% V_2O_5 is obtained from low-intensity wet magnetic separation (LIWMS). The sulfide mineral content is negligible and does not have any significant effect on the processing circuits.

Therefore, in the proposed circuit, an HIDMS is initially used in order to remove diamagnetic impurities from the placer mineral. Then as the heavy minerals are the main constituent of the valuable minerals, the concentrate obtained is transferred to the shaking table for separation of light and heavy particles, and the middling product of the table is returned back to the table for further processing. Since the particle size distribution of the mineral is less than 1000 μm, and most of them are below 500 μm in size, setting the frequency and amplitude for the separation of light and heavy particles is of great importance. Thus by setting the amplitude appropriately, an acceptable separation of heavy particles containing iron minerals is obtained. The conditions used for the shaking table are given in Table 9.

The final concentrate of the table that contains heavy iron minerals with a high magnetic property (magnetite) is subjected to size reduction by a ball mill to under 75 μm for liberating valuable minerals locked with gangue (Table 10). Finally, the comminuted product is introduced to LIWMS to separate magnetic minerals (Table 11). Since magnetite is the main iron-bearing mineral in the sample, a good recovery is obtained by LIWMS, and sulfur and phosphor assay is acceptable for iron- and steel-making processes.

Vanadium is concentrated, and uniformly distributed, in magnetite rather than titanium. The higher content of V_2O_5 in the magnetite lattice can be due to replacing Fe^{3+} for V^{3+}. Thus considering the V_2O_5 content (0.77%), this concentrate is a suitable resource for vanadium production, compared to some vanadium extraction resources in the world.

The Bardaskan placer deposit contains 1% TiO_2, and it is one of the low-grade titanium deposits in the world. The TiO_2 content of the studied deposit is lower than Tellnes (up to 18% TiO_2 and 35% ilmenite) [9] and Otanmäki (up to 14% TiO_2 and 28% ilmenite) [15] ores, and is not comparable with these ores from a reserve viewpoint. The maximum recoverable TiO_2 content of the ore does not exceed 8%. Also much of the titanium and vanadium are disseminated in silicate minerals, and are unrecoverable by physical methods. Thus it cannot be used as an appropriate deposit to extract titanium.

Furthermore, considering the iron recovery of 1.4% with 55% Fe content, despite the complicated mineralogical features of studied ore, it is predicted that by combination of the gravity methods such as shaking table and Humphrey spiral and high intensity magnetic separation and low intensity wet magnetic separation, the concentration and production of iron from the studied deposit is possible, and it can be used in metallurgical factories for steel-making.

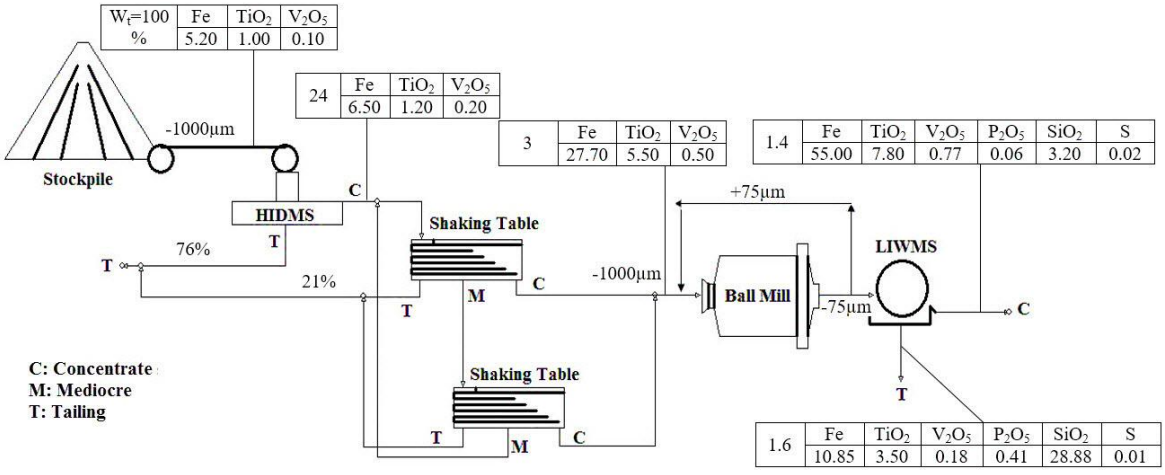

Figure 9. Suggested circuit for iron enrichment from the Bardaskan titanomagnetite deposit.

Table 9. Conditions used for gravity separation.

Situation	Data
Total feed (kg)	480
Mass flow rate (kg/h)	300
Water flow rate (L/h)	1400
Vibration range (mm)	10
Size distribution (mm)	–1
Solid percentage (%)	18

Table 10. Experimental conditions used for grinding.

Situation	Data
Feed (kg)	65
Size distribution (mm)	–1
Solid percentage (%)	35
D80 (µm)	75

Table 11. Conditions used for low intensity wet magnetic separator.

Situation	Data
Feed (kg)	65
Size distribution (µm)	–75
Mass flow rate (g/min)	150
Water flow rate (mL/min)	750
Magnetic intensity (G)	900
Solid percentage (%)	17

4. Conclusions

According to the mineralogical studies, the iron content of the applied placer sample is about 5%, which mostly consists of magnetite, and a little part of it is hematite (formed as a result of martitization). Except for these iron-bearing minerals, much of the deposit is composed of silica and non-iron minerals. Moreover, liberation studies revealed that in order to achieve a better separation between the magnetic and gangue minerals, it is necessary to reduce the particle size to under 75 µm. Using the shaking table, the concentrator with an appropriate frequency and amplitude after the first magnetic separation step effectively removes much of the silicates due to their low density in comparison to the valuable minerals. Concerning the proposed flow sheet and the applied conditions, 55% Fe and 0.77% V_2O_5 extraction with a maximum amount (7.8%) of TiO_2 enrichment is possible. Furthermore, separation of ilmenite from magnetite seems to be impossible, as confirmed by the diffraction map of titanium in the iron bearing minerals obtained by EPMA studies. Therefore, economically speaking, although the Bardaskan deposit cannot be considered as an appropriate source for titanium production with respect to its low titanium grade, production of a commercial magnetite concentrate is possible by the combination of gravity and magnetic separation. On the other hand, V_2O_5 of the concentrate is obtainable as the by-product of the hydro-metallurgical processes.

References

[1]. Hukkanen, E. and Walden, H. (1985). The production of vanadium and steel from titanomagnetites. Int. J. Miner. Process. 15: 89-102.

[2]. Gabra, G. and Malinsky, I. (1981). A comparative study of the extraction of vanadium from titaniferous magnetite and slag. In. Process. Symposium. Extractive Metall. Refract. Met.. 110th AIME Annual Meeting. Chicago. U.S.A. pp. 167-189.

[3]. Jena, B.C., Dresler, W. and Reilly, I.G. (1995). Extraction of titanium, vanadium, and iron from titanomagnetite deposits at pipestone lake. Manitoba. Canada. Miner. Eng. 8: 159-168.

[4]. Battle, T.P., Nguyen, D. and Reeves, J.W. (1993). The processing of titanium-containing ores. In: Reddy, R.G. and Weizenback, R.N., Eds., The Paul E. Queneau International Symposium: Extractive Metallurgy of Copper. Niquel and Cobalt. Vol. 1. TMS. Warrendale. pp. 925-943.

[5]. Kahn, J.A. (1984). Non-rutile feedstocks for the production of titanium. J. Met. 36: 33-38.

[6]. Chernet, T. (1999a). Applied mineralogical studies on australian sand ilmenite concentrate with special reference to its behavior in the sulphate process. Miner. Eng. 12: 485-495.

[7]. Colin, J.D. (2001). Ilmenite, titanium dioxide, and titanium. New Zealand Mining. 30: 30-37.

[8]. Chernet, T. (1994). Ore microscopic investigation of selected Fe-Ti oxides bearing samples from Koivusaarenneva mineralization and other localities in

South Western Finland. Geological Survey of Finland 10, 1-25. Unpublished Report.

[9]. Chernet, T. (1999b). Effect of mineralogy and texture in the TiO_2 pigment production process of the Tellnes ilmenite concentrate. Miner. Petrol. 67: 21-32.

[10]. Mcenroe, S.A., Robinson, P. and Panish, P.T. (2000). Chemical and petrographic characterization of ilmenite and magnetite in oxide-rich cumulates of the Sokndal Region. Rogaland. Norway. NGU Bull. 436: 49-56.

[11]. Kärkkäinen, N. and Appelqvist, H. (1999). Genesis of a low-grade apatite-ilmenite-magnetite deposit in the Kauhajärvi gabbro. Western Finland. Miner. Deposita. 34: 754-769.

[12]. Sarapää, O., Kärkkäinen, N., Chernet, T., Lohva, J. and Ahtola T. (2005). Exploration results and mineralogical studies on the Lumikangas apatite-ilmenite gabbro. Kauhajoki. Western Finland. Geological Survey of Finland. Spec. Pap. 38: 31-40.

[13]. Chernet, T. (1999c). Mineralogical and textural constraints on mineral processing of the Koivusaarenneva ilmenite ore. Kälviä. Western Finland. Int. J. Miner. Process. 57: 153-165.

[14]. Chernet, T. (2003). Applied mineralogical studies on Iso-Kisko ilmenite ore deposit with respect to the ore amenability to beneficiation. Kisko. Southern Finland. Research report. Geological Survey of Finland. Research Laboratory. Espoo.

[15]. Kerkkonen, O. (1979). The magnetite-ilmenite of the Otanmäki titanium iron ore, interpretation of the source and development. PhD Thesis. University of Oulu. Finland.

[16]. Kärkkäinen, N., Sarapää, O., Huuskonen, M., Koistinen, E. and Lehtimäki, J. (1997). Ilmenite exploration in Western Finland, and the mineral resources of the Kälviä deposit. Geological Survey of Finland. Special Paper. 23: 15-24.

[17]. Grammatikopoulos, T., Mcken, A., Hamilton, C. and Christiansen, O. (2002). Vanadium-bearing magnetite and ilmenite mineralization and beneficiation from the Sinarsuk V-Ti project. West Greenland. CIM Bull. 95: 87-95.

[18]. Nantel, S. (2001). The Sept-Iles project-A new apatite/ilmenite producer?. CIM Bull. 94: 59-63.

[19]. Rao, D.S., Vijayakumar, T.V., Prabhakar, S., Bhaskar Raju, G. and Ghosh, T.K. (2005). Alteration characteristics of ilmenites from South India. J. Miner. Mater. Charact. & Eng. 4: 47-59.

[20]. Samanta, S., Mukherjee, S. and Dey, R. (2014). Oxidation behaviour and phase characterization of titaniferous magnetite ore of Eastern India. T. Nonferr. Metal. Soc. 24: 2976-2985.

[21]. Holmes, W.T. and Banning, L.H. (1964). Electric smelting of titaniferous iron ores from Alaska, Montana, and Wyoming. United States Department of the Interior. Bureau of Mines. Report of Investigations 6497.

[22]. Diemer, R.A. (1941). Titaniferous magnetite deposits of the Laramie Range. Wyoming. Genesis 18, 19.

[23]. Mehdilo, A., Irannajad, M. and Rezai, B. (2015). Applied mineralogical characterization of ilmenite

from Kahnuj placer deposit. Southern Iran. Periodico di Mineralogia. 84 (2): 289-302.

[24]. Korneliussen, A., McEnroe, A.S., Nilsson, L.P., Schiellerup, H., Gautneb, H., Meyer, B.G. and Størseth, L.R. (2000). An overview of titanium deposits in Norway. Norges geologiske undersøkelse Bulletin. 436: 27-38.

[25]. Samala, S., Mohapatra, B.K., Mukherjee, P.S. and Chatterjee, S.K. (2009). Integrated XRD, EPMA and XRF study of ilmenite and titanium slag used in pigment production. J. Alloys and Compounds. 474: 484-489.

مطالعات کانی‌شناسی و فراوری فیزیکی به منظور استخراج آهن از نهشته پلاسری تیتانومگنتیتی بردسکن

مصطفی حسین‌زاده[۱*]، مهدی علیزاده[۱] و محمد رئوف حسینی[۲]

۱- پژوهشگاه مواد و انرژی کرج، ایران

۲- بخش مهندسی معدن، دانشگاه صنعتی اصفهان، ایران

ارسال ۲۰۱۶/۱/۱، پذیرش ۲۰۱۶/۸/۷

* نویسنده مسئول مکاتبات: mta.hosseinzadeh@yahoo.com

چکیده:

در این تحقیق، بازیابی آهن از یک نهشته پلاسری واقع در شهرستان بردسکن-استان خراسان رضوی، با استفاده از روش‌های فراوری مواد معدنی در مقیاس آزمایشگاهی مورد مطالعه قرار گرفت. مطالعات کانی‌شناسی انجام شده توسط آنالیزهای پراش اشعه ایکس (XRD)، فلوئورسانس اشعه ایکس (XRF)، میکرو-آنالیزور حسگر الکترونی (EPMA) و میکروسکوپ نوری نشان داد که تیتانومگنتیت، مگنتیت و هماتیت کانی‌های با ارزش موجود در نمونه بودند. در مقابل، سیلیکات‌هایی همچون پیروکسن، پلاژیوکلاز، کوارتز، فلدسپار، کلسیت و برخی کانی‌های ثانویه، به عنوان گانگ‌های موجود در نمونه شناسایی شدند. درجه آزادی بهینه کانی‌های آهن‌دار، حدود ۷۵ میکرون با عیار متوسط آهن ۵٪ و TiO_2 ۱٪ به دست آمد. همچنین، آنالیزها نشان داد که مگنتیت، کانی آهن‌دار اصلی موجود در نمونه بوده و بیشتر هماتیت حاضر در نمونه، در اثر مارتیتیزاسیون تشکیل شده است. به علاوه، مقادیر بسیار کمی از ایلمنیت درون هماتیت و مگنتیت به صورت تیغه‌ای یافت شد. بیشترین مقدار TiO_2 در شبکه مگنتیت، ۱۹٪ بود که ۸٪ آن در محصول مغناطیسی بازیابی شد. در نهایت، فلوشیتی برای تغلیظ آهن ارائه شد که شامل حذف مقادیر زیادی از سیلیکات‌ها و جداسازی کانی‌های آهن‌دار با استفاده از جداکننده مغناطیسی تر شدت پایین بود. محصول نهایی، دارای ۵۵٪ آهن، ۷/۸٪ TiO_2 و ۰/۷۷٪ V_2O_5 بوده است که می‌تواند به منظور تولید آهن و V_2O_5 مورد استفاده قرار گیرد.

کلمات کلیدی: تیتانومگنتیت، مگنتیت، درجه آزادی، آهن، فلوشیت.